Published in final edited form as:
Int J Non Linear Mech. 2013 November ; 58: 79–85. doi:10.1016/j.ijnonlinmec.2013.03.002.

Non-linear micromechanics of soft tissues

Huan Chen[a], **Xuefeng Zhao**[a], **Xiao Lu**[a], and **Ghassan Kassab**[a,b,*]

[a]Department of Biomedical Engineering, Indiana University Purdue University Indianapolis, Indianapolis, IN 46202, United States

[b]Department of Surgery, Cellular and Integrative Physiology, Indiana University Purdue University Indianapolis, Indianapolis, IN 46202, United States

Abstract

Microstructure-based constitutive models have been adopted in recent studies of non-linear mechanical properties of biological soft tissues. These models provide more accurate predictions of the overall mechanical responses of tissues than phenomenological approaches. Based on standard approximations in non-linear mechanics, we classified the microstructural models into three categories: (1) uniform-field models with solid-like matrix, (2) uniform-field models with fluid-like matrix, and (3) second-order estimate models. The first two categories assume affine deformation field where the deformation of microstructure is the same as that of the tissue, regardless of material heterogeneities; i.e., they represent the upper bounds of the exact effective strain energy and stress of soft tissues. In addition, the first type is not purely structurally motivated and hence cannot accurately predict the microscopic mechanical behaviors of soft tissues. The third category considers realistic geometrical features, material properties of microstructure and interactions among them and allows for flexible deformation in each constituent. The uniform-field model with fluid-like matrix and the second-order estimate model are microstructure-based, and can be applied to different tissues based on micro-structural features.

Keywords

Collagenous tissue; Collagen; Elastin; Microstructure; Constitutive relation; Non-affine deformation

1. Introduction

The significance of mechanical stress and strain in biology, physiology and pathology is well recognized. The determination of microstructural stress requires a constitutive model based on the ultrastructure and the corresponding material properties. Complex microstructure and strong non-linear mechanical behaviors of soft tissue, however, present significant challenges in constitutive modeling. Despite the complexity, the current trend in

*Corresponding author at: Department of Biomedical Engineering, Indiana University Purdue University Indianapolis, Indianapolis, IN 46202, United States. Tel.: +1 44 13172748337. gkassab@iupui.edu (G. Kassab).

biomechanics is to move from phenomenological to micromechanical models in order to predict the overall non-linear and microstructural responses of inhomogeneous soft tissues. New developments in imaging and biochemistry will continue to provide more details of the constitutive properties of soft tissues, and continue to advance the development of structure-based models.

This review introduces non-linear structural models of soft tissues including their utility and limitations. A finite strain micromechanics is introduced, and two homogenization methods (upper bound and SOE approach) are provided. Three types of microstructure-based models of soft tissues are compared in relation to their assumptions and micromechanical basis; i.e., (1) uniform-field models with solid-like matrix, (2) uniform-field models with fluid-like matrix, and (3) second-order estimate models.

1.1. Ultrastructure of soft tissues

Biological soft tissues are primarily composed of collagen and elastin fibers, ground substance (GS), and cells. The physiological function of each soft tissue necessitates certain degree of structural anisotropy, which is generally realized by variable arrangements of the functional components. Specifically, fibers can have variable densities and topologies such as orientation, length, width, and degree of undulation. For example, tendon has a uniaxial structure with parallel wavy fibers formed by Type I collagen fibrils [1]. Blood vessels, on the other hand, have three layers (i.e., intima, media, and adventitia) from the lumen to the external surface whose mechanical properties are differentiated by the respective arrangement of collagen and elastin fibers, and cells.

As a primary functional component of soft tissues, collagen fibrils are assemblies of subfibrils of about 30 nm diameter, each consisting of microfibrils packed in a tetragonal lattice. The diameter of collagen fibrils ranges from 50 to 500 nm, depending on tissue type and the age of the animal [1], and these fibrils typically run parallel and gather in large collagen bundles [2,3]. Morphological observations show that collagen fibers have undulated structure and mainly arrange in plane with preferred orientations, which results in anisotropic properties of tendon, ligament, and blood vessels (collagen in blood vessel is shown in Fig. 1a) [4,5]. Collagen bundles have also been found to run in all directions and form a two-dimensional isotropic network in small intestine [2]. The degree of collagen undulation (waviness) is different in soft tissues; e.g., it is very small in tendon (almost straight), larger in the skin and even larger in the mesentery [6]. At lower macroscopic stretch of the tissue, the undulated collagen fibers contribute little or no effect to the mechanical response. As the macroscopic stretch increases, collagen bundles become straightened gradually and eventually bear most of the load to render a highly non-linear stress–strain relationship [2,7]. It is noted that uncoiled collagen fibrils have a Young's modulus of the order of 0.1–1.0 GPa along the fibril direction, whereas the Young's modulus of elastin is of the order of 100 kPa [8–10].

Elastin fibers are straight rod-like fibrils composed of a central core surrounded by microfibrils with a 10 nm diameter [11]. The arrangement of elastin varies among soft tissues. Elastin fibers distribute relatively randomly and form a net-like structure in coronary arteries [2] (Fig. 1b), but uniformly and preferentially orient with collagen fibers in articular

cartilages [12]. Moreover, there are abundant elastin fibers in aortic tissue (more than 40% by dry weight), while tendon contains few elastin fibers (less than 3% by dry weight) [13]. Experimental observations show that elastin fibers gradually extend to take up the load together with cells and GS at very low strain levels [2,7], where the stress–strain behavior of the whole tissue exhibits only weak non-linearity.

The non-fibrous components of soft tissues are GS and cells. GS is an amorphous gel-like structure that mainly contains glycosaminoglycans, proteoglycans and glycoproteins [14,15]. These hydrophilic macromolecules create water-filled compartments that maintain turgor pressures within tissues. In addition, proteoglycans strongly interact with fibers and cells by forming interfibrillar bridges [16,17]. Enzymatic degradation of tissues (specific to GS) shows that the gel-like GS has very low resistance to shear stress and thus has little effect on the mechanical response of tendon, skin and aorta [18,19]. Fibroblasts are the most common cells found in soft tissues, which synthesize and secrete extracellular matrix (ECM, denoting fibers and GS here) and play an important role in healing wounds [20,21]. Smooth muscle cells (SMCs), on the other hand, are only found in vasoactive tissue, such as blood vessel, lymphatic vessel and urinary bladder, where the structure and function of SMC is basically the same. Some studies have shown that cells (fibroblasts and SMCs) have negligible effects on passive mechanical behaviors of tissues [7,22–24]. Other studies, however, suggest that SMCs have a significant role in transmitting stresses through serial connections with collagen fibers [25–28]. The degree of mechanical contribution of SMCs has not been well established, and future studies are needed to resolve this controversy.

The above studies suggest that the mechanical properties of soft tissues largely stem from the microstructural components, and their arrangements determine the functional properties of the resulting structure. Based on these findings, structurally motivated models have become popular [29–34], with the early seminal work of Lanir [5,6].

1.2. Non-linear micromechanics of heterogeneous materials

The idea of homogenization of heterogeneous non-biological materials has been proposed for quite some time to predict the macroscopic or effective mechanical properties of composites [35]. Rigorous and reliable methods have been well established and widely applied to linear elastic composites in academia research and industry, including the classical Voigt and Reuss bounds [36], the variational principles of Hashin–Shtrikman [37,38], and the general self-consistent approximations [39,40]. For non-linear composites, however, rigorous methods have become available only recently because of difficulties in addressing both strong material non-linearity and heterogeneity. Earlier efforts were made to predict the effective constitutive behaviors of composites by extending linear methods to non-linear materials, such as the extensions of the self-consistent procedures [41], or the Hashin–Shtrikman variational principles for linear composites [42,43].

A general variational procedure for estimating the effective behavior of non-linear composites was proposed by Ponte Castañeda [44]. He introduced a “linear elastic comparison composite” (LCC) with the same microstructure of the non-linear composite, which allows for the use of numerous bounds and estimates for linear composites. Ponte Castañeda further proposed an alternative approach with more sophisticated LCC to

generate estimates that are exact to the second-order in the phase contrast [45,46]. This is the so-called second-order estimate (SOE) homogenization, which yields significant improvements over previous micromechanics models. During the past decade, successive developments have been made to the SOE approach by Ponte Castañeda and his colleagues to better predict the non-linear macroscopic properties of heterogeneous materials [29,47–53]. Applications have been extended to various non-linear materials with randomly or periodically distributed microstructure, including viscoplastic polycrystal, porous or reinforced rubbers and fiber-reinforced elastomers. Moreover, the SOE model was recently applied to biological fibrous tissue by Chen et al. [29], to describe the micro- and macroscopic mechanical behaviors of soft tissues.

2. Framework of non-linear micromechanics

Finite strain micromechanics can be used to determine the macroscopic constitutive response of biological soft tissues based on structural and mechanical properties of microstructure. Based on the principle of minimum strain energy, the framework can provide multiple approximate solutions for macroscopic strain energy function (SEF) of soft tissues. An “upper bound” and a “second-order” estimate models are discussed below.

2.1. Hyperelastic heterogeneous material

A heterogeneous material, such as soft tissue, is made up of $N + 1$ ($N \geq 1$) different phases, which are distributed (randomly or with a certain distribution of orientation or dimension) in a specimen with a volume Ω and boundary $\partial\Omega$ in the reference configuration. The constitutive behavior of each inclusion is characterized by a respective SEF $W^{(r)}(\mathbf{F})$, so that the local SEF $W(\mathbf{X},\mathbf{F})$ of composites is written as:

$$W(\mathbf{X},\mathbf{F})=\sum_{r=0}^{N}\chi^{(r)}(\mathbf{X})W^{(r)}(\mathbf{F}), \quad (1)$$

where $\mathbf{F}$ is defined as the deformation gradient tensor, and $\chi^{(r)} = 1$ when $\mathbf{X}\in\Omega^{(r)}$ (the volume occupied by phase r), or 0 otherwise to describe the distribution of the microstructure. The local stress field (i.e., the microscopic constitutive behavior) of the inhomogeneous material is expressed, based on thermodynamics, as:

$$\mathbf{S}(\mathbf{X})=\frac{\partial W(\mathbf{X},\mathbf{F})}{\partial\mathbf{F}}-p\mathbf{F}^{-T}. \quad (2)$$

It should be noted that $\mathbf{S}(\mathbf{X})$ is the first Piola-Kirchhoff stress tensor, which is related to the Cauchy stress tensor $\boldsymbol{\sigma}$ by $\mathbf{S} = \boldsymbol{\sigma}\cdot\mathbf{F}^{-T}$, and the hydrostatic stress p is due to incompressibility ($\det(\mathbf{F}) = 1$) of the soft tissue.

According to the principle of minimum strain energy, the effective SEF of a microscopically inhomogeneous hyperelastic material is defined as previously [54–56] by

$$\bar{W}(\bar{\mathbf{F}})=\min_{\mathbf{F}\in\kappa(\bar{\mathbf{F}})}\langle W(\mathbf{X},\mathbf{F})\rangle=\min_{\mathbf{F}\in\kappa(\mathbf{F})}\sum_{r=0}^{N}c^{(r)}\langle W^{(r)}(\mathbf{F})\rangle^{(r)}, \quad (3)$$

where the brackets $\langle\cdot\rangle$ and $\langle\cdot\rangle^{(r)}$ denote volume averages over the composite Ω and over the r-th phase $\Omega^{(r)}$, respectively, so that $c^{(r)} = \langle\chi^{(r)}\rangle$ represents the volume fraction of the r-th phase. $\kappa(\bar{\mathbf{F}}) = \{\mathbf{F}|\mathbf{F}(\mathbf{X}) = \mathbf{I} + \nabla_{\mathbf{X}}\mathbf{u}(\mathbf{X})$ in Ω, and $\mathbf{u}(\mathbf{X}) = (\bar{\mathbf{F}}-\mathbf{I}) \cdot \mathbf{X}$ on $\partial\Omega\}$ denotes all the admissible deformation gradient field in the representative volume element (RVE) of the composite with an affine displacement boundary condition $\mathbf{u}(\mathbf{X})$. In analogy with the local expression of Eq. (2), assuming sufficient smoothness for $\bar{W}(\bar{\mathbf{F}})$, the macroscopic stress of the composite is defined by

$$\bar{\mathbf{S}}=\frac{\partial\bar{W}(\bar{\mathbf{F}})}{\partial\bar{\mathbf{F}}} - p\bar{\mathbf{F}}^{-T}, \quad (4)$$

where $\bar{\mathbf{S}} = \langle\mathbf{S}\rangle$ and $\bar{\mathbf{F}} = \langle\mathbf{F}\rangle$, which are also called as the average stress and average deformation gradient, respectively. The effective SEF $\bar{W}$ physically represents the average elastic energy stored in the composite. In general, the rigorous minimization solution for Eq. (3) is difficult to obtain for a heterogeneous material with complex microstructure since a set of highly non-linear partial differential equations must be solved. Consequently, approximate solutions or estimates have been pursued [41–46,51,53]. The efforts to seek an approximate minimizing field $\mathbf{F}(\mathbf{X})$ have resulted in several classes of finite strain micromechanics models including the uniform-field upper bound and the second-order estimate.

2.2. Uniform-field upper bound model

The simplest trial field for Eq. (3) is $\mathbf{F}(\mathbf{X}) = \bar{\mathbf{F}}$, which assumes a uniform deformation field in the composite. As a consequence, the macroscopic SEF $\bar{W}(\bar{\mathbf{F}})$ is simply the volumetric sum of the constituents,

$$\bar{W}(\bar{\mathbf{F}}) \approx \bar{W}_U(\bar{\mathbf{F}})=\sum_{r=0}^{N} c^{(r)}W^{(r)}(\bar{\mathbf{F}}). \quad (5)$$

This solution leads to an upper bound of the exact SEF $\bar{W}$ as $\bar{\mathbf{F}}$ is an admissible deformation field that does not minimize the total strain energy. It is usually referred to as the Voigt upper bound in linear micromechanics. Consequently, the effective stress $\bar{\mathbf{S}}_U = \partial\bar{W}_U/\partial\bar{\mathbf{F}} - p\bar{\mathbf{F}}^{-T}$ is an upper bound of the exact macroscopic stress for a given $\mathbf{F}$. This approximation requires that all phases must deform with the same deformation regardless of their different material properties (e.g., stiffness). This assumption is not true for composites that have widely different phases. In addition, the affine deformation assumption only includes information on the phase volume fraction $c^{(r)}$ (as indicated by Eq. (5)), but neglects the interactions between phases that may affect the overall mechanical response of a composite.

2.3. s-order estimate approach

A second-order homogenization approach, utilizing the concept of an LCC, was proposed by Ponte Castañeda [45,46]. This method has been widely applied to non-linear elastomeric composites, including reinforced and porous elastomers, as well as other heterogeneous elastomeric systems [47,51,52]. This approach accounts for the statistical microstructure beyond the volume fraction of the phases and incorporates interactions amongst different

phases. Hence, it provides a more accurate prediction of the constitutive behavior of non-linear composites than the uniform-field upper bound.

Following derivation in Refs. [51,53], an LCC is introduced with effective SEF $\bar{W}_T(\bar{\mathbf{F}})=\sum_{r=0}^{N}\chi^{(r)}(\mathbf{X})W_T^{(r)}(\mathbf{F})$ to denote that it has the same microstructure as the non-linear composites, but each of the phases is linearly elastic with the SEF $W_T^{(r)}$ (i.e., the second-order Taylor approximation to the non-linear SEF $W^{(r)}$). According to generalized Legendre transform of the strain energy [51,53], the exact macroscopic SEF expressed in Eq. (3), can be approximated by:

$$\bar{W}(\bar{\mathbf{F}}) \leq \min_{\{\mathbf{F}^{*(s)},\mathbf{L}^{(s)}\}}\{\bar{W}_T(\bar{\mathbf{F}};\{\mathbf{F}^{*(s)},\mathbf{L}^{(s)}\})+\sum_{r=0}^{N}c^{(r)}V^{(r)}(\mathbf{F}^{*(r)},\mathbf{L}^{(r)})\}, \quad (6)$$

where $\mathbf{L}^{(r)}$ is the unknown reference modulus and $\mathbf{F}^{*(r)}$ is the virtual residual deformation gradient of the r-th phase of LCC, both of which will be determined by the minimization procedure of Eq. (6). $V^{(r)}(\mathbf{F}^{*(r)},\mathbf{L}^{(r)})=\sup_{\hat{\mathbf{F}}}\{W^{(r)}(\hat{\mathbf{F}})-W_T^{(r)}(\hat{\mathbf{F}})\}$ is a "corrector" function; i. e., the error induced by approximating the non-linear composite SEF $W^{(r)}$ with the SEF of LCC $W_T^{(r)}$. This approximation translates the optimization over continuous deformation field $\mathbf{F}\in\boldsymbol{\kappa}(\bar{\mathbf{F}})$ to the modulus tensor, $\mathbf{L}^{(r)}$, and the deformation gradient tensor, $\mathbf{F}^{*(r)}$, of the r-th phase of composite (r varies from 0 to N). In theory, the field $\mathbf{F}\in\boldsymbol{\kappa}(\bar{\mathbf{F}})$ must satisfy the continuity and compatibility conditions, while $\mathbf{L}^{(r)}$ and $\mathbf{F}^{*(r)}$ can be arbitrary within the physically meaningful ranges. Although $\mathbf{L}^{(r)}$ and $\mathbf{F}^{*(r)}$ are allowed to change from point to point in the material, we assume that they are uniform for the r-th phase based on standard non-linear micromechanics [52,53,57].

The work of Ponte Castañeda and Willis [45] suggested that replacing the minimization over the variables $\mathbf{L}^{(r)}$ and $\mathbf{F}^{*(r)}$ in Eq. (6) by the corresponding stationary points yields a stationary estimate, and thus generates a so-called "second-order estimate" for the exact SEF of the non-linear composites. The stationary procedures involved in the above derivation (maximization of $V^{(r)}$ and the minimization in Eq. (6)) yield a set of non-linear tensorial equations for the determination of the unknown reference modulus $\mathbf{L}^{(r)}$ and the reference deformation gradient $\mathbf{F}^{*(r)}$[51,53,58]. These equations have multiple solutions that lead to various estimations of the macroscopic SEF $\bar{W}(\bar{\mathbf{F}})$. A *tangent* solution is widely used for composites with complex microstructure, in which the reference deformation gradient is taken to be the average deformation gradient; i.e., $\mathbf{F}^{*(r)} = \bar{\mathbf{F}}^{(r)}$ in the r-th phase of the LCC, and $\mathbf{L}^{(r)}$ is the tangent stiffness tensor evaluated at $\mathbf{F}^{(r)}$ [59]. This solution leads to $V^{(r)}(\mathbf{F}^{*(r)}, \mathbf{L}^{(r)}) = 0$ and an estimate of $\bar{W}(\bar{\mathbf{F}})$ as

$$\bar{W}(\bar{\mathbf{F}}) \approx \bar{W}_S(\bar{\mathbf{F}})=\sum_{r=0}^{N}c^{(r)}\left\{W^{(r)}(\bar{\mathbf{F}}^{(r)})+\frac{1}{2}\boldsymbol{\rho}^{(r)}(\bar{\mathbf{F}}^{(r)})(\bar{\mathbf{F}}-\bar{\mathbf{F}}^{(r)})\right\}, \quad (7)$$

where $\boldsymbol{\rho}^{(r)}$ is used to denote the first derivation of the phase potential $W^{(r)}$; i.e., $\boldsymbol{\rho}^{(r)}(\bar{\mathbf{F}}^{(r)}) = (\partial W^{(r)}/\partial\mathbf{F})_{\mathbf{F}=\bar{\mathbf{F}}^{(r)}}$. In order to compute this estimate, the effective strain energy $\bar{W}_T(\mathbf{F})$ and the average deformation gradient of phases $\bar{\mathbf{F}}^{(r)}$ of the LCC are determined by extended

finite strain Hashin–Shtrikman theory [48,60] which takes into account the stiffness $\mathbf{L}^{(r)}$ as well as the shape and distribution of the composite phases [29,51,53].

The advantage of this method is that it can be used for any type of non-linear composite and is capable of dealing with the strongly non-linear constraint of material incompressibility, which is relevant for biological soft tissues. The SOE model statistically accounts for the heterogeneous deformation in composites (i.e., $\bar{\mathbf{F}}^{(r)}$ varies in phases), which is due to the heterogeneities of microstructural geometries and material properties, as well as interactions amongst constituents. The deformation field is therefore more realistic than that of the upper bound solution. Consequently, SOE leads to more accurate estimates of the macroscopic SEF and stress for the composites, as well as microscopic stress for microstructure, as compared with the upper bound solution.

3. Micromechanical models for soft tissues

Numerous microstructural constitutive models of soft tissues have been proposed in the past several decades that proved to be more accurate than previous phenomenological models. Three major types of these micromechanical models are classified based on various assumptions and approximations in non-linear micromechanics as described below.

3.1. Uniform-field models based on a solid-like matrix

The first class of micromechanical models was motivated by anisotropic mechanical behaviors of soft tissues. Previous studies showed that the elastin becomes straightened and starts to take load in the early deformation of the tissue as an isotropic material. For instance, the experimental study of Gundiah et al. [10] suggested that the elastin can be well described by isotropic neo-Hookean constitutive model. Meanwhile, collagen fibers, with preferred orientation, are largely associated with the anisotropic response of soft tissues [61]. Based on these observations, the tissue is considered as a collagen fiber reinforced composite with a solid-like matrix that can bear load. As proposed by Holzapfel et al. [31], the SEF of non-collagenous matrix material, including elastin fibers, cells and GS (matrix defined here is not the same as ECM), W_M, is associated with the isotropic deformation, and the SEF of collagen W_C is related to the anisotropic part due to the deformation of two families of collagen fibers. Hence, the effective SEF of tissue is the sum of these two functions:

$$\bar{W}(\bar{\mathbf{C}})=W_M(\bar{\mathbf{C}})+W_C(\bar{\mathbf{C}},\mathbf{N}_1,\mathbf{N}_2), \quad (8a)$$

$$W_M(\bar{\mathbf{C}})=A_1(\bar{I}_1-3), W_C(\bar{\mathbf{C}},\mathbf{N}_1,\mathbf{N}_2)=\frac{k_1}{2k_2}\sum_{i=4,6}\{\exp[k_2(\bar{I}_i-1)^2]-1\}, \quad (8b)$$

where $\mathbf{N}_1$ and $\mathbf{N}_2$ are the direction vectors of the two families of collagen fibers, A_1 is a material parameter associated with elastin fiber, k_1 is a material parameter associated with collagen fiber and k_2 is a dimensionless parameter [31]. The right Cauchy–Green deformation tensor $\bar{\mathbf{C}}$ is related to the deformation gradient by $\bar{\mathbf{C}} = \bar{\mathbf{F}}^T \cdot \bar{\mathbf{F}}$. The first invariant

of $\bar{\mathbf{C}}$ is $\bar{I}_1 = tr(\bar{\mathbf{C}})$, and the fourth and sixth invariants are $\bar{I}_4 = \mathbf{N}_1 \cdot \bar{\mathbf{C}} \cdot \mathbf{N}_1$ and $\bar{I}_6 = \mathbf{N}_2 \cdot \bar{\mathbf{C}} \cdot \mathbf{N}_2$, respectively.

This model, where the uniform-field approximation $\mathbf{F}(\mathbf{X}) = \bar{\mathbf{F}}$ is employed (as in Eq. (8)), presents an upper bound of the exact effective SEF of soft tissue. In addition, the direction vectors $\mathbf{N}_1$ and $\mathbf{N}_2$ of fibers were determined by empirical curve fitting rather than based on histological observations [31]. Given that fiber orientation follows a certain continuous distribution in biological tissues [4,62], these two parameters are phenomenological variables rather than structural parameters. Moreover, engagement of undulated collagen fibers (characterized by the fiber waviness distribution) is described by an exponential SEF W_C, and thus is also phenomenological. In order to obtain more accurate predictions, this model has been subsequently revised. Zulliger et al. [34] refined the model by accounting for not only the wavy nature of collagen fibers but also the volume fraction of both elastin and collagen, based on different SEFs of the matrix and collagen fibers. Kroon and Holzapfel [63] later incorporated this model into multi-layered structures with the mean fiber alignments in various layers. Li and Robertson [32] also extended this model to account for either a finite number of fiber orientations or a fiber distribution function. In summary, the mechanical predictions of these models are more accurate than those of phenomenological models because they reflect the heterogeneity of material properties and some of the geometrical features of tissues. These models, however, cannot accurately predict the microenvironment (strain and stress of individual fiber or cell) of soft tissues, since they assume affine deformation in tissue and use non-histological based microstructure.

3.2. Uniform-field models based on a fluid-like matrix

The second class of micromechanical models is structurally motivated, and was proposed based on the following assumptions: (1) fibers are thin and flexible with only tensile strength (i.e., fibers cannot resist compressive load); (2) fibers are embedded in a fluid-like matrix, of which the mechanical contribution is only via hydrostatic pressure; (3) the second assumption leads to a simplification that all the microstructure deform identically to the macroscopic deformation of the tissue (i.e., uniform deformation) since no fiber–fiber interactions are considered. On the basis of these assumptions and thermodynamic consideration, Lanir developed a general multi-axial theory for the constitutive relations in fibrous connective tissues [5,6,64]. In his model [6], an important structural feature is the density distribution function of the fiber orientation $R_i(\mathbf{N})$ where $\mathbf{N}$ is a unit vector tangent to the fiber. Thus $R_i(\mathbf{N})\Delta\Theta$ is the volumetric fraction of fibers of type i (classified by waviness and fiber type) which are oriented in direction $\mathbf{N}$ and occupy a spatial angle $\Delta\Theta$. According to previous derivation for uniform-field models, the macroscopic SEF in this model is the volumetric sum of the SEF of fibers in all directions:

$$\bar{W}(\bar{\mathbf{F}}) = \sum_i \sum_{\mathbf{N}} c^{(i)} W^{(i)}(\lambda_f) \cdot R_i(\mathbf{N}) \cdot \Delta\Theta, \quad (9)$$

where $c^{(i)}$ is the volumetric fraction of unstrained fibers of type i, and $W^{(i)}(\lambda_f)$ is the fiber SEF of type i, which depends on fiber stretch ratio $\lambda_f = \sqrt{\mathbf{N} \cdot (\bar{\mathbf{F}}^T \cdot \bar{\mathbf{F}}) \cdot \mathbf{N}}$. This equation is

identical to Eq. (5) as $\sum_{\mathbf{N}} c^{(i)} R_i(\mathbf{N}) \Delta\Theta$ denotes the volumetric fraction of a particular fiber phase with the type *i* SEF and orientation **N** in soft tissues. The SEF of fiber $W^{(i)}(\lambda_f)$ and the density distribution function $R_i(\mathbf{N})$ are specific to different tissue types, of which microstructural geometries and material properties may be determined by histological and mechanical measurements. This model can account for geometrical distributions (e.g., orientation, waviness, etc.) as well as the mechanical response of single fibers, but it assumes affine deformation and neglects inter-fiber interactions due to the assumption of a fluid-like matrix.

The fluid-like matrix assumption was also employed by Decraemer et al. [65] to develop a parallel wavy fibers model for soft biological tissues in uniaxial tension, assuming a normal distribution for initial length of fibers (i.e., fiber waviness). Wuyts et al. [33] extended this model by utilizing a Lorentz distribution function for the initial fiber length. In summary, the fluid-like matrix models are more rational than the solid-like matrix models because they involve structural and constitutive behaviors of both functional constituents of soft tissues: collagen and elastin. The basic fluid-like matrix assumption may be an accurate description for certain tissues where the non-fibrous constituents are mainly fibroblasts, macrophage and amorphous gel-like GS that do not take up significant non-hydrostatic loading. These micromechanical models with fluid-like matrix have been widely applied to different soft tissues, including tendon [66], skin [67,68], myocardium [69] and more recently in blood vessels [30].

3.3. SOE models based on solid-like matrix

Recently, a finite strain micromechanical model (based on the aforementioned SOE approach) was developed by Chen et. al. [29] to predict the macroscopic stress–strain relation and microstructural deformation of soft fibrous tissue. This model showed significant improvements over previous microstructure models when compared to finite element method (FEM) simulations. In this model, the tissue is considered as a composite with reinforcing fibers and soft solid matrix (Fig. 2). The orientation of the *r*-th fiber is described by $\Theta^{(r)}$, the shape (dimension) is described by a geometric tensor $\mathbf{Z}^{(r)}$, and the spatial distribution of the *r*-th fiber is characterized by another geometric tensor $\boldsymbol{Z}_d^{(r)}$ while the waviness is included in the SEF of the *r*-th fiber to reflect fiber recruitment under macroscopic tissue deformation. Specifically, a piecewise function was used to describe the constitutive behavior of a single fiber:

$$W^{(r)}(\mathbf{F}) = \begin{cases} W^{(0)}(\mathbf{F}) & \lambda_f < \lambda_0^{(r)}, \\ W^{(0)}(\mathbf{F}) + W_{fiber}^{(r)}(\lambda_f) & \lambda_f \geq \lambda_0^{(r)}, \end{cases} \quad (10)$$

where λ_f is the fiber stretch ratio, $\lambda_0^{(r)}$ is the waviness of the *r*-th fiber, and $W^{(0)}$ denotes the SEF of the matrix. This function implies that a fiber deforms the same as the soft matrix before straightening, and becomes stiffer with additional SEF of fiber $W_{fiber}^{(r)}$ after straightening (as shown in Fig. 2b). The matrix was described by a neo-Hookean SEF, while the anisotropic term $W_{fiber}^{(r)}(\lambda)$ in the SEF of fibers was selected as:

$$W_{fiber}^{(r)}(\lambda_f)=E_1(\lambda_f-\lambda_0^{(r)})^2/2+E_2(\lambda_f-\lambda_0^{(r)})^3/3, \quad (11)$$

where E_1, E_2 are material parameters of individual fibers. This is a generalization of the linear model employed in other works [5,6,33,65] where only the first term $(\lambda_f-\lambda_0^{(r)})^2$ was included. In principle, the homogenization model employed in this work can use any well-defined constitutive models of the matrix and fibers.

By substituting fiber geometrical features $\mathbf{G}^{(r)}(\boldsymbol{Z}^{(r)},\boldsymbol{Z}_d^{(r)},\theta^{(r)},\lambda_0^{(r)})$ and mechanical properties (Eqs. (10) and (11)) into Eqs. (6) and (7), and utilizing the finite strain Hashin–Shtrikman theory [29,48], the macroscopic SEF and stress of soft tissue as well as microscopic deformation $\bar{\mathbf{F}}^{(r)}$ of every component can be obtained through solving multiple non-linear equations [29,52]. It should be noted that the microscopic deformation $\bar{\mathbf{F}}^{(r)}$ of the *r*-th fiber is not identical to either the macroscopic tissue deformation or other fiber phases since the admissible deformation field $\mathbf{F}(\mathbf{X})$ is not $\bar{\mathbf{F}}$ (as in the uniform-field models) and is determined by tissue inhomogeneity. As compared with the first two model types, this micromechanical model not only considers realistic geometrical features and material properties of tissue constituents and their interactions, but also allows flexible deformation in each constituent. Hence, the model is an actual estimate rather than an upper bound of the exact effective SEF, and provides a more accurate prediction of the macroscopic and microscopic mechanical behavior of the soft tissue.

3.4. Comparison between the uniform-field and SOE models

A comparison was made between the uniform-field model with solid-like matrix (first class) and the SOE model (third class), where elastin was considered as the matrix along with GS and cells, and collagen was the reinforcing phase. The fiber orientation and waviness were assumed to follow beta-distributions [62], with the latter being direction-dependent in line with tissue ultrastructure (the mean of collagen waviness was taken to be 1.6) [66,70].

The model predictions showed that at low stretch level ($\bar{\lambda} < 1.6$), most fibers remain undulated and deform the same as the matrix so that the predictions of uniform-field and SOE models are similar (Fig. 3a). With increase of the tissue deformation ($\bar{\lambda} > 1.6$), the uniform-field predictions rise rapidly while SOE results increase slowly in line with FEM results (Fig. 3a). At this loading level, collagen fibers become completely straightened to take up loads and deform less than the matrix. The uniform-field model, however, overestimates the deformation field of stiffer fibers (assumes it is identical to that of the matrix) and hence approaches the upper bound. The SOE model statistically accounts for the heterogeneous deformation of the matrix and fibers, which is due to the heterogeneities of microstructural geometries and material properties as well as matrix–fiber and fiber–fiber interactions. Thus, the deformation field employed by SOE is more realistic and leads to lower estimates of the macroscopic SEF and stress than the uniform-field upper bound. In addition, the statistical deformation of each constituent largely depends on both fiber orientation and waviness, as predicted by the SOE model (Fig. 3b and c). The microscopic deformation is non-affine once some fibers are straightened and become stiffer to take up

load. For fibers with a low waviness or larger orientation angle, they deform less (after recruited) than other phases even at very large macroscopic deformation. The uniform-field predictions only depend on the orientation angle but not the waviness, based on affine deformation assumption.

The microstructural SOE model, however, is more computational costly than the uniform-field model with solid-like matrix. Hence, the predictive capability of uniform-field and SOE models under various conditions was investigated to assess the tradeoff between computational cost and accuracy. The present *tangent* SOE approach requires a set of $9(N + 1)$ non-linear equations $\mathbf{F}^{*(r)} = \bar{\mathbf{F}}^{(r)}$, where $\mathbf{F}^{(r)}$ takes into account the stiffness $\mathbf{L}^{(r)}$ as well as the shape and distribution of the composite phases [29,51,53], and an equation for the effective SEF (Eq. (6)), while the uniform-field model only requires a simple volumetric sum of the SEF of constituents (Eq. (5)). The computational cost of SOE model is approximately 20 times that of the uniform-field model. Moreover, it was found that the shape and distribution of microstructure were found to have significant influence on model predictions [29]. For instance, the SOE macroscopic Cauchy stress of fibrous tissue with aligned fibers is similar to the uniform-field prediction. It appears that the uniform-field model with solid matrix is accurate for soft tissue with very narrow distribution of fiber orientation. Direct comparison was not made between the SOE model and the uniform-field model with fluid-like matrix because the assumption of the matrix properties is different in the two models. The fluid-like matrix may be appropriate for some tissues, such as tendon which is predominated by collagen (occupies more than 80% by dry weight [13]). For other tissues, such as the media layer of a blood vessel where elastin and collagen fibers form a complex network connected to vascular SMC, of which the cytoskeleton (actin, myosin, tubulin, etc.) has significant contribution to mechanical loading [25,26] and thus can sustain non-hydrostatic loading such as tension and shear. The applicability of the fluid-like matrix assumption to various tissues requires further investigations.

4. Summary

This review classifies the majority of microstructural models of biological soft tissues into three major types, according to various assumptions and approximations in non-linear micromechanics. In general, the recently developed SOE model (third type) can provide the most accurate predictions of macroscopic and microscopic mechanical behaviors for soft tissues but with significant computational cost. The uniform-field model with a fluid-like matrix (second type) assumes affine deformation in soft tissue and neglects fiber–fiber interactions based on the fluid-like matrix assumption and is much less computationally costly. The choice of constitutive models for soft tissues can depend on whether the matrix (GS and cells) is fluid-like or solid-like. Accurate quantitative data of microstructure are needed to construct the structural models (both for second and third classes). Thus, the modeling developments point to the need for morphometric data and constitutive behaviors of tissue components. Furthermore, with increasing interest in micro-environment of soft tissues in physiology and pathology, the full microstructural model with capabilities to predict heterogeneous microscopic stress and deformation is a laudable goal for the near future.

References

1. Hiltner A, Cassidy JJ, Baer E. Mechanical properties of biological polymers. Annual Review of Materials Science. 1985; 15:455–482.
2. Ottani V, Raspanti M, Ruggeri A. Collagen structure and functional implication. Micron. 2001; 32:251–260. [PubMed: 11006505]
3. Birk DE, Trelstad RL. Extracellular compartments in tendon morphogenesis: collagen fibril, bundle, and macroaggregate formation. The Journal of Cell Biology. 1986:231–240. [PubMed: 3722266]
4. Chen H, Liu Y, Slipchenko MN, Zhao XF, Cheng JX, Kassab GS. The layered structure of coronary adventitia under mechanical load. Biophysical Journal. 2011; 101:2555–2562. [PubMed: 22261042]
5. Lanir Y. A structural theory for the homogeneous biaxial stress-strain relationships in flat collagenous tissues. Journal of Biomechanics. 1979; 12:423–436. [PubMed: 457696]
6. Lanir Y. Constitutive equations for fibrous connective tissues. Journal of Biomechanics. 1983; 16:1–12. [PubMed: 6833305]
7. Roach MR, Burton AC. The reason for the shape of the distensibility curves of arteries. Canadian Journal of Biochemistry and Physiology. 1957; 35:681–690. [PubMed: 13460788]
8. Burton AC. Relation of structure to function of the tissues of the wall of blood vessels. Physiological Reviews. 1954; 34:619–642. [PubMed: 13215088]
9. Gosline J, Lillie M, Carrington E, Guerette P, Ortlepp C, Savage K. Elastic proteins: biological roles and mechanical properties. Philosophical Transactions of the Royal Society B: Biological Sciences. 2002; 28:121–132.
10. Gundiah N, Ratcliffe MB, Pruitt LA. Determination of strain energy function for arterial elastin: experiments using histology and mechanical tests. Journal of Biomechanics. 2007; 40:586–594. [PubMed: 16643925]
11. Montes GS. Structural biology of the fibres of the collagenous and elastic systems. Cell Biology International. 1996; 20:15–27. [PubMed: 8936403]
12. Mansfield J, Yu J, Attenburrow D, Moger J, Tirlapur U, Urban J, Cui Z, Winlove P. The elastin network: its relationship with collagen and cells in articular cartilage as visualized by multiphoton microscopy. Journal of Anatomy. 2009; 215:682–691. [PubMed: 19796069]
13. Holzapfel, GA. Biomechanics of soft tissue. In: Lemaitre, J., editor. Handbook of Material Behavior Models. USA: Academic press; 2001. p. 1057-1071.
14. Eisenstein R, Larsson SE, Kuettner KE, Sorgente N, Hascal VC. The ground substance of the arterial wall. Part 1. Extractability of glycosaminoglycans and the isolation of a proteoglycan from bovine aorta. Atherosclerosis. 1975; 22:1–17. [PubMed: 125595]
15. Gogiel T, Jaworski S. Proteoglycans of human umbilical cord arteries. Acta Biochimica Polonica. 2000; 47:1081–1091. [PubMed: 11996098]
16. Scott JE, Thomlinson AM. The structure of interfibrillar proteoglycan bridges (‘shape modules’) in extracellular matrix of fibrous connective tissues and their stability in various chemical environments. Journal of Anatomy. 1998; 192:391–405. [PubMed: 9688505]
17. Wight, TN. Arterial wall. In: Comper, D., editor. Extracellular Matrix, Tissue Function. Vol. 1. Amsterdam: Harwood Academic Pulishers GmbH, W.; 1996. p. 175-202.
18. Oxlund H, Andreassen TT. The roles of hyaluronic acid, collagen and elastin in the mechanical properties of connective tissues. Journal of Anatomy. 1980; 131:611–620. [PubMed: 7216901]
19. Viidik A, Danielso CC, Oxlund H. On fundamental and phenomenological models, structure and mechanical properties of collagen, elastin and glycosaminoglycan complexes. Biorheology. 1982; 19:437–451. [PubMed: 6286009]
20. McAnulty RJ. Fibroblasts and myofibroblasts: their source, function and role in disease. The International Journal of Biochemistry & Cell Biology. 2007; 39:666–671. [PubMed: 17196874]
21. Rhee S, Grinnell F. Fibroblast mechanics in 3D collagen matrices. Advanced Drug Delivery Reviews. 2007; 59:1299–1305. [PubMed: 17825456]
22. Thoumine O, Ott A. Time scale dependent viscoelastic and contractile regimes in fibroblasts probed by microplate manipulation. Journal of Cell Science. 1997; 110:2109–2116. [PubMed: 9378761]

23. Wolinsky H, Glagov S. Structural basis for the static mechanical properties of the aortic media. Circulation Research. 1964; 14:400–413. [PubMed: 14156860]
24. Cox RH. Passive mechanics and connective tissue composition of canine arteries. American Journal of Physiology-Heart and Circulatory Physiology. 1978; 234:533–541.
25. Roy S, Tsamis A, Prod'hom G, Stergiopulos N. On the in-series and in-parallel contribution of elastin assessed by a structure-based biomechanical model of the arterial wall. Journal of Biomechanics. 2008; 41:737–743. [PubMed: 18456913]
26. Roy S, Silacci P, Stergiopulos N. Biomechanical properties of decellularized porcine common carotid arteries. American Journal of Physiology-Heart and Circulatory Physiology. 2005; 289:1567–1576.
27. Silver FH, Snowhill PB, Foran DJ. Mechanical behavior of vessel wall: a comparative study of aorta, vena cava, and carotid artery. Annals of Biomedical Engineering. 2003; 31:793–803. [PubMed: 12971612]
28. Sokolis DP, Kefaloyannis EM, Kouloukoussa M, Marinos E, Boudoulas H, Karayannacos PE. A structural basis for the aortic stress-strain relation in uniaxial tension. Journal of Biomechanics. 2006; 39:1651–1662. [PubMed: 16045914]
29. Chen H, Liu Y, Zhao XF, Lanir Y, Kassab GS. A micromechanics finite-strain constitutive model of fibrous tissue. Journal of the Mechanics and Physics of Solids. 2011; 59:1823–1837. [PubMed: 21927506]
30. Hollander Y, Durban D, Lu X, Kassab GS, Lanir Y. Experimentally validated microstructural 3D constitutive model of coronary arterial media. Journal of Biomechanical Engineering. 2011; 133:031007. [PubMed: 21303183]
31. Holzapfel GA, Gasser TC, Ogden RW, New A. Constitutive framework for arterial wall mechanics and a comparative study of material models. Journal of Elasticity. 2000; 61:1–48.
32. Li D, Robertson AM. A structural multi-mechanism constitutive equation for cerebral arterial tissue. International Journal of Solids and Structures. 2009; 46:2920–2928.
33. Wuyts FL, Vanhuyse VJ, Langewouters GJ, Decraemer WF, Raman ER, Buyle S. Elastic properties of human aortas in relation to age and atherosclerosis: a structural model. Physics in Medicine and Biology. 1995; 40:1577. [PubMed: 8532741]
34. Zulliger MA, Fridez P, Hayashi K, Stergiopulos N. A strain energy function for arteries accounting for wall composition and structure. Journal of Biomechanics. 2004; 37:989–1000. [PubMed: 15165869]
35. Milton, GW. The Theory of Composites. Cambridge: Cambridge University Press; 2002.
36. Hill R. The elastic behaviour of a crystalline aggregate. Proceedings of the Physical Society. Section A. 1952; 65:349–354.
37. Hashin Z, Shtrikman S. A variational approach to the theory of the elastic behaviour of multiphase materials. Journal of the Mechanics and Physics of Solids. 1963; 11:127–140.
38. Hashin Z, Shtrikman S. A variational approach to the theory of the elastic behaviour of polycrystals. Journal of the Mechanics and Physics of Solids. 1962; 10:343–352.
39. Hershey A. The elasticity of an isotropic aggregate of anisotropic cubic crystals. Journal of Applied Mechanics-Transactions ASME. 1954; 21:236–240.
40. Hutchinson JW. Bounds and self-consistent estimates for creep of polycrystalline materials. Proceedings of the Royal Society A. 1976; 348:101–127.
41. Hill R. A self-consistent mechanics of composite materials. Journal of the Mechanics and Physics of Solids. 1965; 13:213–222.
42. Talbot DRS, Willis JR. Variational principles for inhomogeneous non-linear media. IMA Journal of Applied Mathematics. 1985; 35:39–54.
43. Willis JR. The overall elastic response of composite materials. Journal of Applied Mechanics. 1983:1202.
44. Ponte Castañeda P. The effective mechanical properties of nonlinear isotropic composites. Journal of the Mechanics and Physics of Solids. 1991; 39:45–71.
45. Ponte Castañeda P, Willis JR. Variational second-order estimates for non-linear composites. Proceedings of the Royal Society A. 1999; 455:1799–1811.

46. Ponte Castañeda P. Exact second-order estimates for the effective mechanical properties of nonlinear composite materials. Journal of the Mechanics and Physics of Solids. 1996; 44:827–862.
47. Agoras M, Lopez-Pamies O, Ponte Castañeda P. A general hyperelastic model for incompressible fiber-reinforced elastomers. Journal of the Mechanics and Physics of Solids. 2009; 57:268–286.
48. Kailasam M, Ponte Castañeda P, Willis JR. The effect of particle size, shape, distribution and their evolution on the constitutive response of nonlinearly viscous composites. I. Theory. Philosophical Transactions: Mathematical, Physical and Engineering Sciences. 1997; 355:1835–1852.
49. Liu Y, Gilormini P, Ponte Castañeda P. Variational self-consistent estimates for texture evolution in viscoplastic polycrystals. Acta Materialia. 2003; 51:5425–5437.
50. Liu Y, Ponte Castañeda P. Second-order theory for the effective behavior and field fluctuations in viscoplastic polycrystals. Journal of the Mechanics and Physics of Solids. 2004; 52:467–495.
51. Lopez-Pamies O, Ponte Castañeda P. On the overall behavior, microstructure evolution, and macroscopic stability in reinforced rubbers at large deformations: I—Theory. Journal of the Mechanics and Physics of Solids. 2006; 54:807–830.
52. Lopez-Pamies O, Ponte Castañeda P. Second-order estimates for the macroscopic response and loss of ellipticity in porous rubbers at large deformations. Journal of Elasticity. 2004; 76:247–287.
53. Ponte Castañeda P. Second-order homogenization estimates for nonlinear composites incorporating field fluctuations: I—theory. Journal of the Mechanics and Physics of Solids. 2002; 50:737–757.
54. Hill R. On constitutive macro-variables for heterogeneous solids at finite strain, Proceedings of the Royal Society A: Mathematical. Physical and Engineering Sciences. 1972; 326:131–147.
55. Hill R, Rice JR. Elastic potentials and the structure of inelastic constitutive laws. SIAM Journal on Applied Mathematics. 1973; 25:448–461.
56. Ogden RW. Extremum principles in non-linear elasticity and their application to composites I: Theory. International Journal of Solids and Structures. 1978; 14:265–282.
57. Willis JR. Bounds and self-consistent estimates for the overall properties of anisotropic composites. Journal of the Mechanics and Physics of Solids. 1977; 25:185–202.
58. Lopez-Pamies O, Ponte Castañeda P. Second-order homogenization estimates incorporating field fluctuations in finite elasticity. Mathematics and Mechanics of Solids. 2004; 9:243–270.
59. Ponte Castañeda P, Tiberio E. A second-order homogenization method in finite elasticity and applications to black-filled elastomers. Journal of the Mechanics and Physics of Solids. 2000; 48:1389–1411.
60. Liu, Y. Ph.D. Dissertation. Philadelphia: University of Pennsylvania; 2003. Macroscopic Behavior, Field Fluctuations and Texture Evolution in Visoplastic Polycrystals.
61. Holzapfel GA, Weizsäcker HW. Biomechanical behavior of the arterial wall and its numerical characterization. Computers in Biology and Medicine. 1998; 28:377–392. [PubMed: 9805198]
62. Sacks MS. Incorporation of experimentally-derived fiber orientation into a structural constitutive model for planar collagenous tissues. Journal of Biomechanical Engineering. 2003; 125:280. [PubMed: 12751291]
63. Kroon M, Holzapfel GA. A new constitutive model for multi-layered collagenous tissues. Journal of biomechanics. 2008; 41:2766–2771. [PubMed: 18657813]
64. Lanir Y. A microstructure model for the rheology of mammalian tendon. Journal of Biomechanical Engineering. 1980; 102:332–339. [PubMed: 6965197]
65. Decraemer WF, Maes MA, Vanhuyse VJ. An elastic stress-strain relation for soft biological tissues based on a structural model. Journal of Biomechanics. 1980; 13:463–468. [PubMed: 7400174]
66. Sverdlik A, Lanir Y. Time-dependent mechanical behavior of sheep digital tendons, including the effects of preconditioning. Journal of Biomechanical Engineering. 2002; 124:78–84. [PubMed: 11871608]
67. Lokshin O, Lanir Y. Viscoelasticity and preconditioning of rat skin under uniaxial stretch: microstructural constitutive characterization. Journal of Biomechanical Engineering. 2009; 131:031009. [PubMed: 19154068]
68. Lokshin O, Lanir Y. Micro and macro rheology of planar tissues. Biomaterials. 2009; 17:3118–3127. [PubMed: 19324407]

69. Horowitz A, Lanir Y, Yin FC, Perl M, Sheinman I, Strumpf RK. Structural three-dimensional constitutive law for the passive myocardium. Journal of Biomechanical Engineering. 1988; 110:200–207. [PubMed: 3172739]

70. Brown IA. A scanning electron microscope study of the effects of uniaxial tension on human skin. British Journal of Dermatology. 1973; 89:383–393. [PubMed: 4759952]

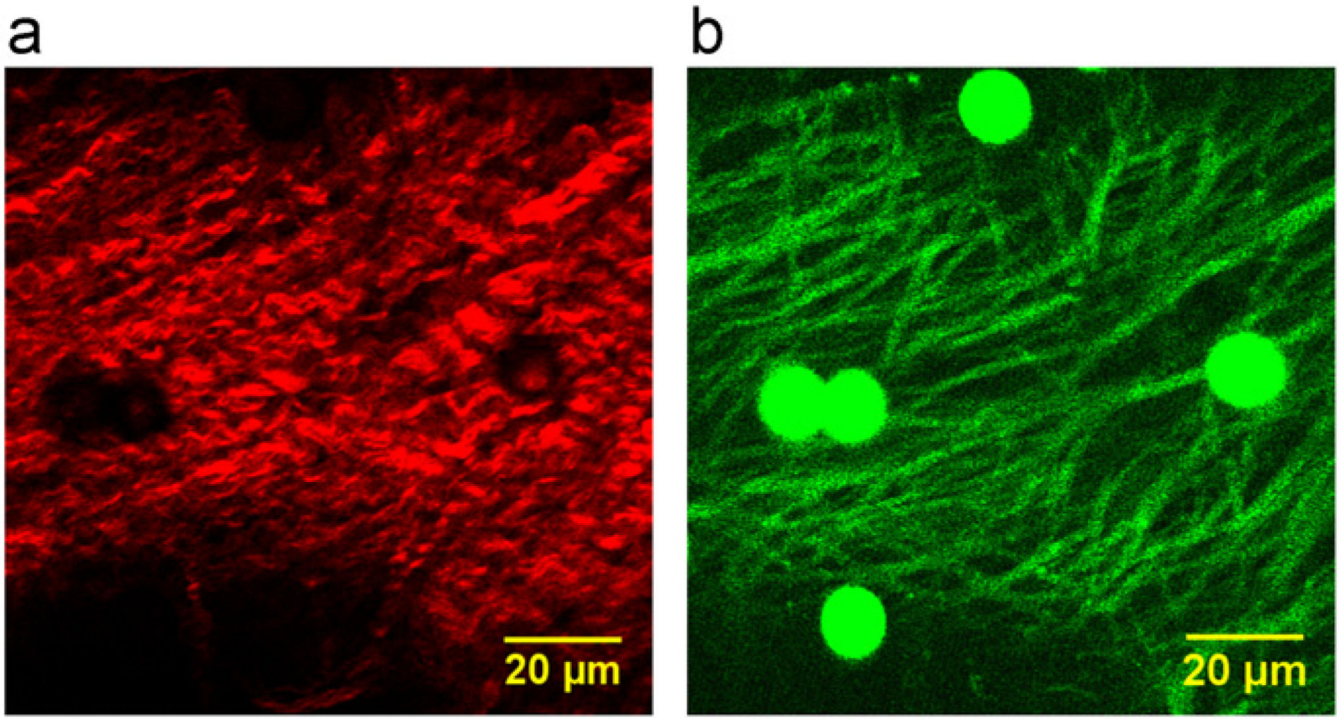

Fig. 1.

Morphometry of collagen and elastin fibers of coronary artery adventitia: (a) Paralleled collagen fibers collected in SHG image; (b) Net-like elastin fibers collected in TPEF image. The Figure is reproduced from Ref. [4].

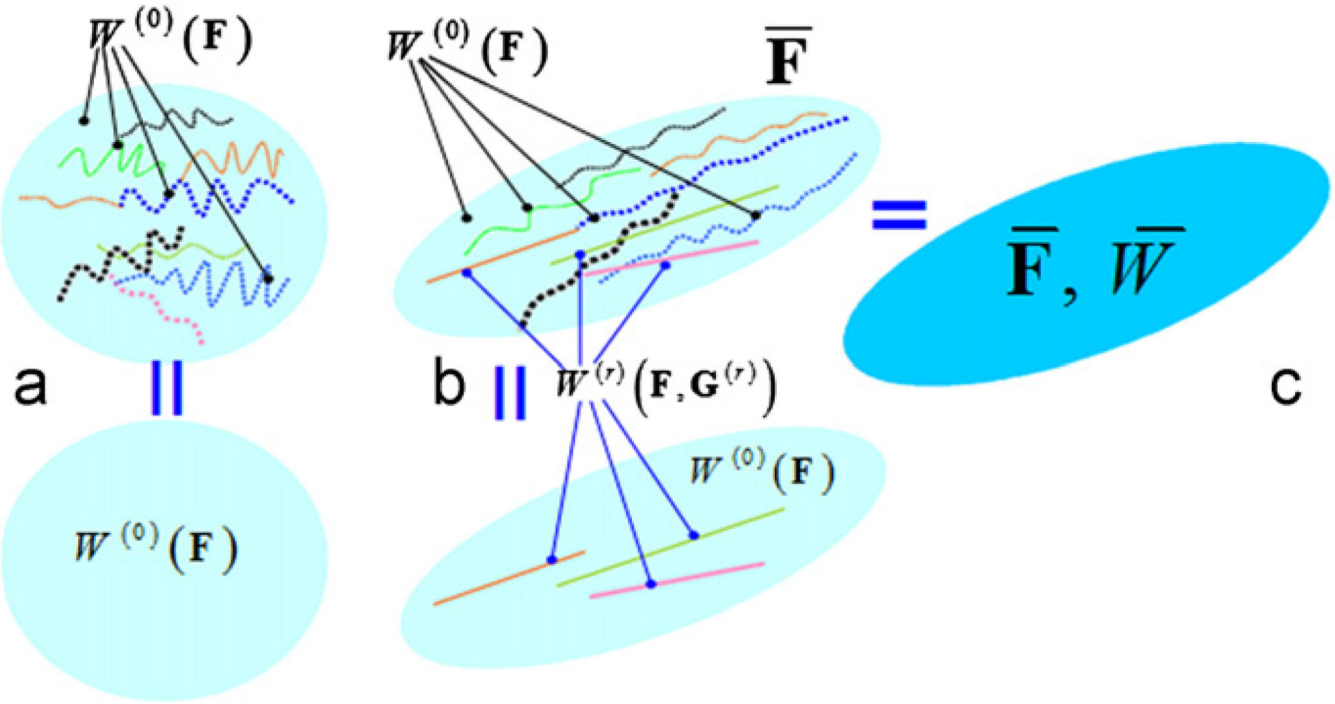

Fig. 2.

Conceptual demonstration of the SOE method. (a) A representative volume element of a fibrous tissue at reference state. All the fibers are undulated and exhibit the same property as the matrix with strain energy function (SEF) W_0; (b) When subjected to a macroscopic $\bar{\mathbf{F}}$, some fibers are straightened and show stiffer property with SEF $W^{(r)}$ as in Eq. (10). (c) The effectively homogeneous material with macroscopic SEF $\bar{W}$. The Figure is reproduced from Ref. [29].

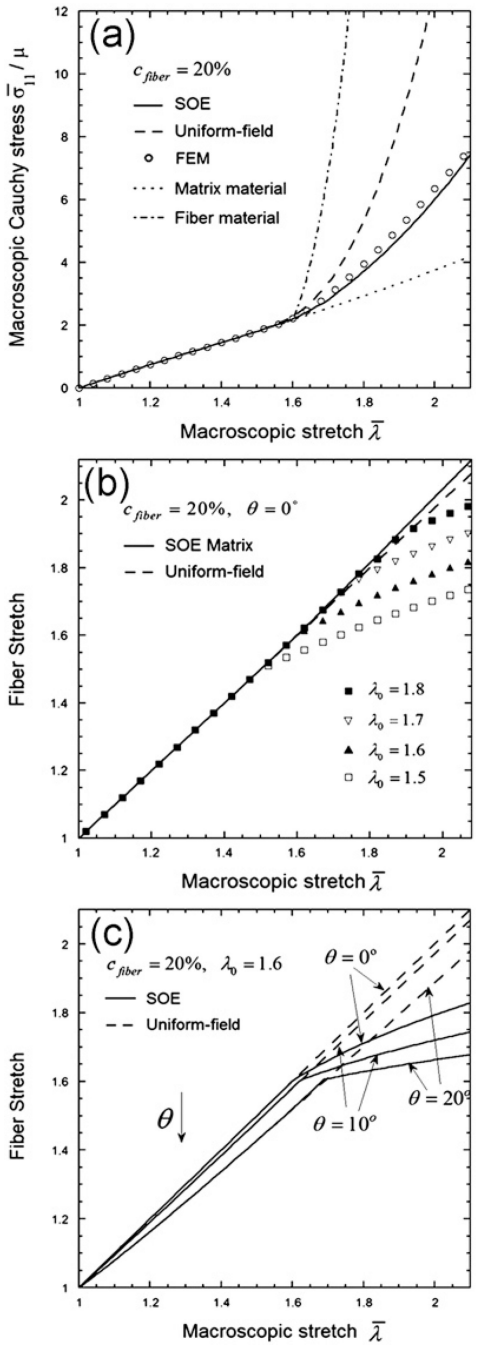

Fig. 3.

Comparisons between the uniform-field model with solid-like matrix and the SOE model: (a) Cauchy stress-stretch relation of soft tissue with 20% randomly distributed collagen fibers; (b) the axial stretch of collagen fibers that are parallel to the loading axis ($\theta = 0°$) depending on waviness λ_0; (c) the axial stretch of collagen fibers with waviness $\lambda_0 = 1.6$ depending on orientation angle θ. The Figure is reproduced from Ref. [29].